Noname manuscript No.
(will be inserted by the editor)

Large Eddy Simulation of Nanosecond Repetitively Pulsed Discharges for the Control of Thermoacoustic Instabilities

D. Maestro[†] · **F. Di Sabatino**[§]
D. Lacoste[§] · **B. Cuenot**[†]

Received: date / Accepted: date

Abstract The effect of nanosecond repetitively pulsed discharges (NRP) on a swirl-stabilized lean premixed methane-air burner has been investigated. A phenomenological model of the NRP behavior and its effect on the gas has been built and implemented in the 3D LES code AVBP. The model is based on experimental measurements done at KAUST and considers, as a first step, the plasma discharge as a simple heating source. Large Eddy Simulations of the experimental burner have been performed with and without NRP discharges, showing how the thermal effect of the plasma triggers chemical reactions and promotes ignition. As observed in the experiment, this leads to a less lifted and more stable flame.

Keywords Large Eddy Simulation · Nanosecond Repetitively Pulsed discharges · Thermoacoustic instabilities · Combustion control

1 Introduction

The need of reduction in fuel consumption and pollutant emissions has lead to an evolution of combustion chambers architectures of gas turbine engines over the past decades. The desired reduction of the fuel/air ratio obliged to move from a rich-quench-lean (RQL) combustion mode towards lean-premixed-prevaporized (LPP) systems. LPP systems have proven significant gain in the emission of CO and NO_x and are used nowadays in ground systems for the production of electrical energy as well as in aeronautical jet engines, using gaseous and liquid fuel respectively.
The lean premixed combustion regime typical of these system makes them subject to some severe drawbacks mainly of dynamical nature. Among them, a particularly critical effect is linked to thermoacoustic oscillations, which can cause severe damage to the engine [3,13]. Such combustion instabilities are the result of an unsteady coupling between the flame heat release rate fluctuations and the combustion chamber acoustics. They are generally found at a particular frequency, corresponding to an acoustic mode of the combustion chamber. Thermoacoustic oscillations can lead to fluctuations in engine thrust and heat transfer at walls, flame blow-off or flashback, causing an early aging of critical system components and in extreme cases even the mechanical failure of the engine.
Unfortunately, combustion instabilities are a phenomenon that is not yet fully understood and the scientific community as well as engine manufacturers put important efforts in trying to build models and systems to predict and avoid them. A strategy to control thermoacoustic instabilities is the so-called "passive control" [8,18]: mechanical components, Helmholtz resonators for instance, designed to damp acoustic oscillations in the combustion chamber are added to the system. This can

D. Maestro
CERFACS - 42 Avenue Gaspard Coriolis, 31057 Toulouse Cedex 01, France
Tel.: +33(0)5 61 19 30 89
E-mail: maestro@cerfacs.fr

[†] *CERFACS - 42 Avenue Gaspard Coriolis, 31057 Toulouse Cedex 01, France*
[§] *King Abdullah University of Science and Technology, Clean Combustion Research Center, Thuwal, Saudi Arabia*

however be done only for particular frequencies identified in the design phase and adds complexity and weight to the system. An alternative approach is to use "active control" techniques, which aim at suppressing the coupling between flame and acoustics by means of sensors and actuators. Among others, nanosecond repetitively pulsed (NRP) plasma discharges have been found to be a possible way to enhance combustion and limit thermoacoustic instabilities. NRP discharges can help ignition [16], increase the lean blow-off limit [17,2] and stabilize the flame [14,11]. All these effects are related to thermal and chemical interactions between the plasma and the fluid [22].
Starting from the work of Lacoste et al. [10], who used NRP discharges to stabilize a premixed swirled methane-air flame, this works has the objective of numerically reproduce this effect, by including a purely phenomenological NRP discharges plasma model in the Large Eddy Simulation (LES) code AVBP [20,7], developed by CERFACS and IFPEN. In order to evaluate separately the contributions of the thermal and chemical effects generated by the plasma on the flame, a NRP model which only considers the gas heating due to the plasma discharge is first developed and used.
The paper is structured as follows: first the experimental configuration is presented in section 2, then the phenomenological NRP discharges model is detailed in section 3. Numerical setup for the LES is summarized in section 4 and results are discussed in section 5.

2 Experimental setup

The experimental setup used for the present study is shown in Fig. 1. It is composed of a burner

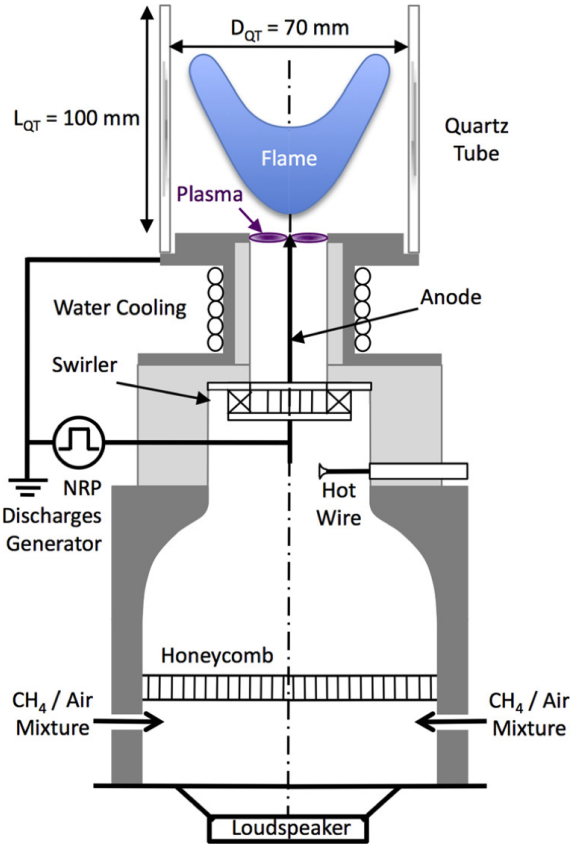

Fig. 1: Experimental burner equipped with a swirler and a NRP discharges system [10]

which produces a swirl stabilized flame and an NRP discharges generator system. Extensive diagnostics are present, for flame transfer function (FTF) measurement and flame visualization, including OH^* chemiluminescence. A mixture of methane and air at an equivalence ratio of 0.67 is fed to the swirl-stabilized burner by means of a mixing chamber. The mixture is injected into a

120 mm long plenum by means of two tubes and passes through a 20 mm long honeycomb in order to break up large turbulent structures. The flow passes through a radial swirler before entering a 18 mm diameter injection tube. The swirler is composed of 12 identical blades with a trailing edge angle of 30 degrees. The main axial velocity of the flow at the exit of the injection tube is about 7 m/s. The flame, featuring a thermal power of about 4 kW, is confined by a quartz tube with an inlet diameter of 70 mm and a length of 100 mm. In order to perform acoustically pulsed calculations, the burner is equipped with a loudspeaker at the bottom end of the plenum.
The NRP discharges generation system is a cylindrical pin steel electrode, 2.5 mm in diameter, located at the center of the injection tube and serving as the anode, while the outlet of the injection tube is used as the cathode. In order to force the plasma discharge location at the outlet of the injection tube, a ceramic cylinder is placed for isolation, leaving only the last 1.5 mm of the injection tube available for the discharge. The electrical pulses are 8 kV in amplitude, 10 ns in duration and have a frequency of 30 kHz. The total power of the plasma is 40 W, i.e. 1 % of the flame power.

3 Phenomenological NRP discharges model

NRP discharges generate and sustain a non-equilibrium plasma state in the gas [9], with electronic temperatures (∼10000 K) much higher than the gas temperature (∼1000 K). In this situation a large number of electronically and vibrationally excited states co-exist, with collisions between electrons and other molecules much more efficient than in equilibrium plasma. This generates various effects on the gas, that are of thermal, chemical and mechanical nature. Thermally, the gas is subjected to an ultra-fast heating of ∼1000 K; moreover there is an ultra-fast excitation of vibrational states of molecules, which later relax towards equilibrium, generating a slow heat source. In addition, ultra-fast dissociation of species occurs with a huge production of molecular oxygen (O). This creates new possible "low temperature" reaction paths for the fuel oxidation [21]. The ultrafast deposition of energy leads to an increase of temperature and pressure in the plasma channel: shock waves form, which can interact with the flame front, increasing its wrinkling and accelerating it [23].
The modeling of a non-equilibrium plasma can be done in different ways, more or less accurate. The approach mostly found in the literature is to use a detailed plasma chemistry coupled with the combustion chemistry. In this case the chemical and thermal non-equilibrium processes are fully coupled and solved. The code must include detailed plasma reactions, electron impact excitation and ionization and relaxation of the excited states. An example of this type of approach can be found in Bak et al. [1]. Although accurate, this approach is too costly to be used in a classical combustion LES code and is limited mostly to direct numerical simulations (DNS) and often in 2D domains.
An alternative approach is to build a phenomenological model based on numerical and experimental observations. A promising example can be found in Castela et al. [4], where a model has been built and used in 2D and 3D DNS. The model is based on the analysis of the distribution of the electrical power over the different energy modes and how excited states impact the thermo-chemical state of the gas when they relax.
In this work a phenomenological model has been developed for practical systems and implemented in the AVBP code. The model is based on experimental observations made at the King Abdulla University of Science and Technology (KAUST, Saudi Arabia). As a first step, the model considers the NRP plasma discharge as a simple heating source. The model is schematically presented in Fig. 2. The energy is supplied to the gas for a time duration of 10 ns, equal to the experimental deposition time, and with a frequency of 30 kHz. Based on experimental data of shape the energy deposit has been fixed as cylindrical, with a 2D gaussian distribution in the cross section of the cylinder (plane y-z in Fig. 2). The cylinder "radius" has been fixed based on the gaussian full width at half maximum (FWHM), which has been set to 500 μm. The distribution has been kept constant along the axis of the cylinder (x axis in Fig. 2), and has been smoothed at both ends by means of an hyperbolic tangent profile. The distribution in the y-z plane reads:

$$\phi(y,z) = \frac{1}{2\pi\sigma^2} \cdot \exp\left[-\frac{1}{2}\left(\frac{y-y_0}{\sigma}\right)^2\right] \cdot \exp\left[-\frac{1}{2}\left(\frac{z-z_0}{\sigma}\right)^2\right] \quad (1)$$

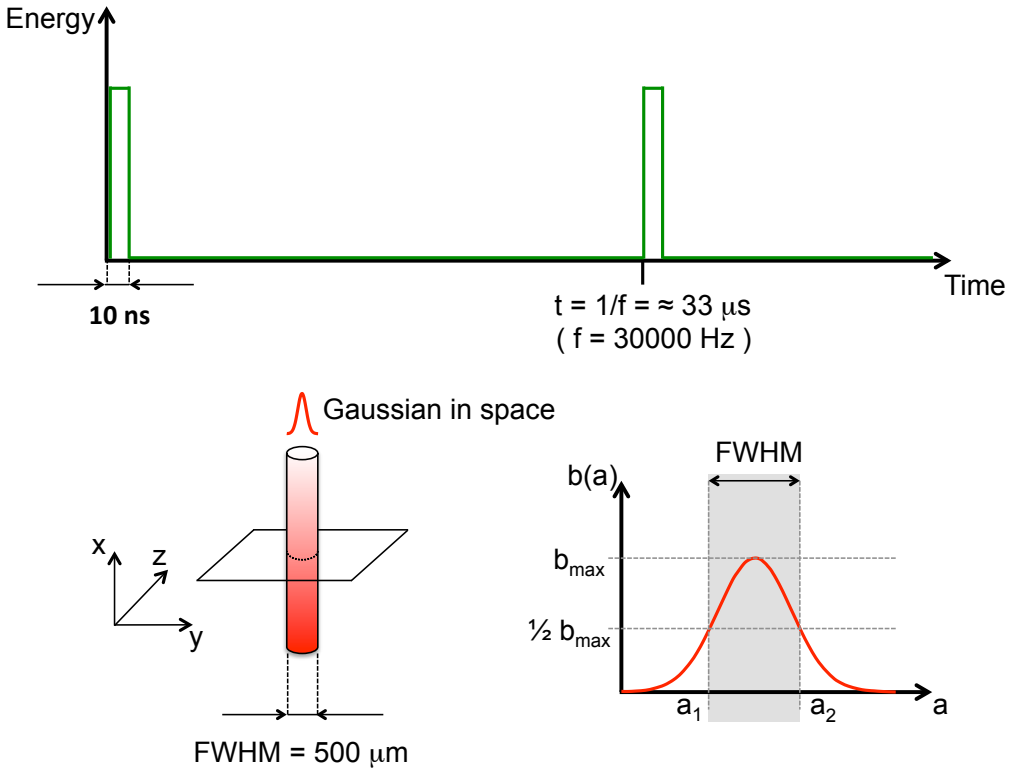

Fig. 2: Schematical representation of the NRP discharges model. Top row: temporal evolution of the energy deposited by the plasma. Bottom row, left: spacial distribution of the plasma channel. Bottom row, right: definition of the gaussian Full Width at Half Maximum (amplitude b as a function of the generic spatial coordinate a)

being the standard deviation $\sigma = \mathrm{FWHM}/2\sqrt{2\ln(2)}$ and (y_0, z_0) the deposition center.
Two perpendicular 2D cuts of the 3D field of the energy deposited by a discharge, non-dimensionalized by its maximum value, are shown in Fig. 3.

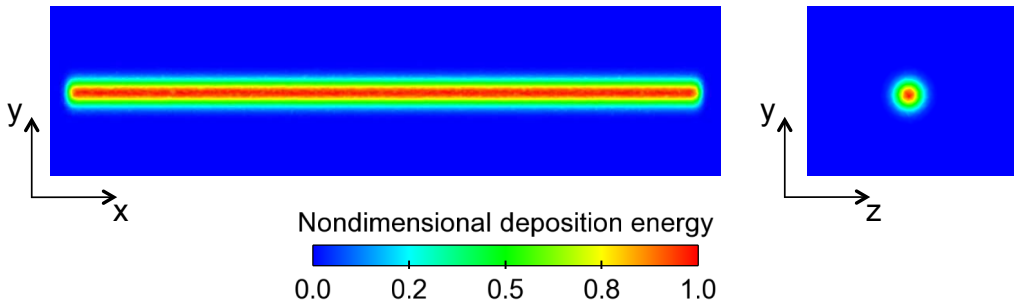

Fig. 3: Field of the energy deposited by an NRP discharge, non-dimensionalized by its maximum value

A key point in the model construction has been to choose where the NRP discharges have to be positioned, considering that they could potentially appear anywhere between the pin steel electrode and the cylindrical inner wall of the injection tube. It has been experimentally observed that the first discharge appears in the inter-electrodes zone of lowest gas density, creating an OH^* filament. Then successive discharges (usually between 2 and 5) at close location increase the OH^* filament intensity, until the latter is too bent by the axial flow to sustain. When this happens, the next discharge takes place at a completely different position, again in the inter-electrodes zone of lowest gas density, and the sequence repeats. Similarly to the flame, the plasma discharges statistically rotate with the swirl.
Following these observations, the numerical discharges model makes them turn around the burner

axis as follows: three consecutive discharges take place next to each other, moving by an angle (θ in Fig. 4) equal to the one of the circle arc traveled by the fluid at the mean azimuthal speed at the exit of the injection tube. After three discharges a random jump in θ appears, in order to mimic the

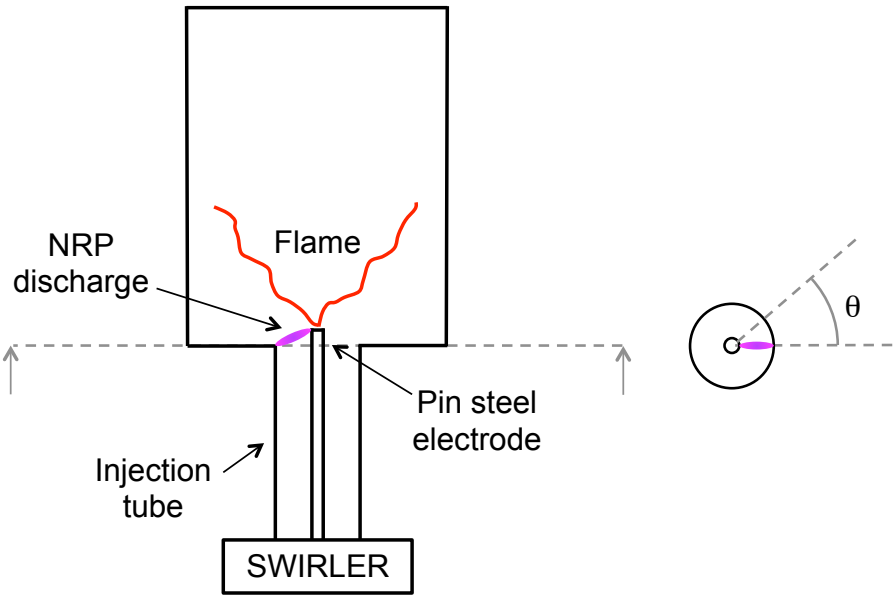

Fig. 4: Position of the NRP discharges

new sudden change of position of the new filament observed experimentally. The following three consecutive discharges stay close to each other, moving with the flow exactly as the first motion series. Then another jump appears, and so on. The number of three close consecutive discharges has been chosen because it is in the experimental range of 2 to 5 discharges observed in the same zone. It is also the number that in validation test cases provides the final gas temperature closest to the experiment (around 3000 K [11]). The jump in θ has been limited between 0 and 180 degrees, to have a statistical motion in the sense of the swirl rotation.

4 LES numerical setup

The computational domain used for the LES simulations is the full three-dimensional burner, starting 25 mm before the inlet of the swirler and extending up to the end of the quartz tube. The domain is discretized with an unstructured mesh entirely composed of thetrahedral cells. The mesh size and the boundary conditions are however different depending on the type of numerical simulation performed. A total of three different numerical simulations have been realized: a cold simulation with the burner fed with only air, an hot reacting simulation without NRP discharges and an hot reacting simulation with NRP discharges. The mesh characteristics and boundary conditions are the following:

– **Cold simulation.** The domain is discretized with a mesh of about 12M of cells (left in Fig. 5). A particular attention has been put to the swirler discretization, where at least 10 cells per vain are used (center, bottom in Fig. 5). This strategy permits to use a wall-of-the-law approach and to limit the mesh size. A mesh refinement is adopted also at the exit of the injection tube, in order to correctly solve the recirculating flow due to vortex breakdown. Moreover the mesh refinement has been adapted to the presence of a flame to allow the use of the same mesh for the cold and hot simulation without NRP discharges. The experimental mass flow rate of pure air is prescribed at inlet with an NSCBC [19] formalism, used also to impose the atmospheric pressure at outlet. Walls are treated as adiabatic and a law-of-the-wall formalism is used everywhere.

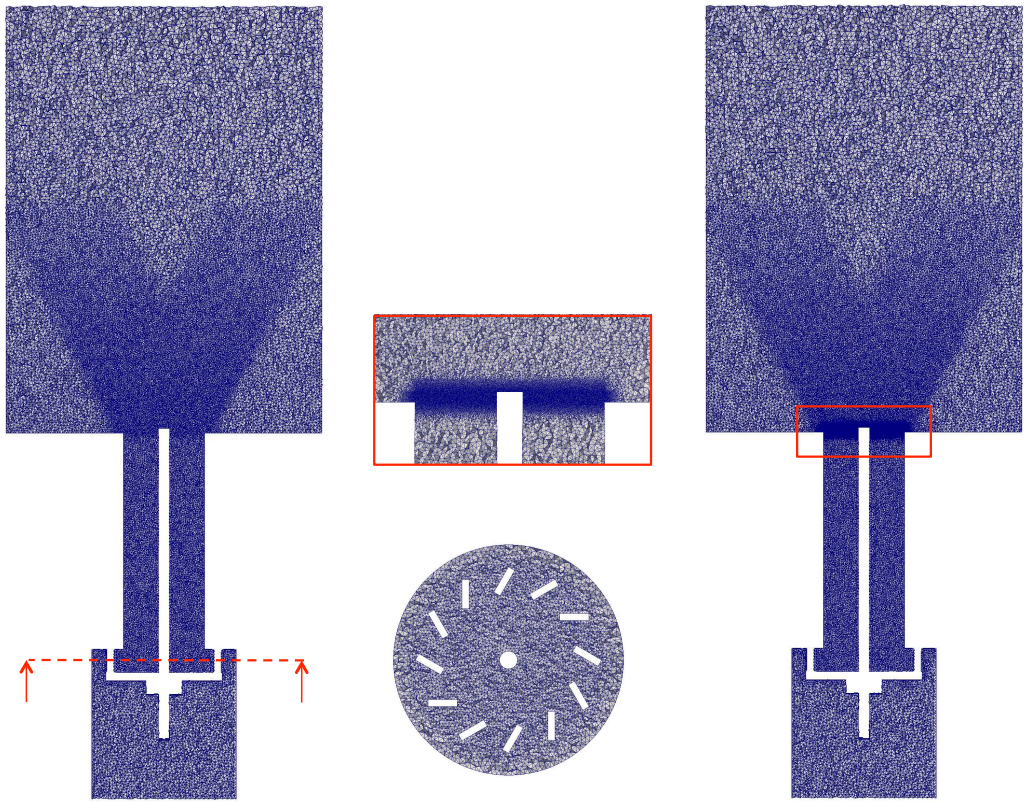

Fig. 5: Cuts of the mesh used for the numerical simulations. Left: mesh used for the cold and hot simulations without NRP discharges. Right: mesh used for the hot simulation with NRP discharges. Center, bottom: mesh in the swirler. Center, top: zoom in the refined zone for NRP discharges.

- **Hot simulation without NRP discharges.** The same mesh as in the cold case is used. The mass flow rate of premixed methane-air used in the experiment is prescribed at inlet. An isothermal formalism for the law-of-the-wall is used for the quartz walls, faceplate and pin steel electrode. The temperature imposed are the one experimentally measured, i.e. 515-610 K for the quartz tube, 515 K for the bottom part of the combustion chamber, and 494 K for the top of the central rod. This permits to avoid the prediction of a totally wrong flame shape: it has been found indeed how this flame is strongly subject to thermal losses at walls, which can make them transition from V-shaped to M-shaped.
- **Hot simulation with NRP discharges.** In order to correctly deposit the energy due to the NRP discharge and solve the formation and propagation of the shock wave around it, a mesh refinement is necessary in the deposition zone (center, top in Fig. 5). A parametric study indicated that 10 points in the gaussian deposit are needed, leading to a mesh size $\Delta \mathrm{x} = 50\ \mu\mathrm{m}$. The mesh is composed of 32M thetrahedral cells (right in Fig. 5). The boundary conditions are the same as for the case without NRP discharges.

The numerical scheme used for the simulations is TTGC [5], third order accurate in space and time. The sub-grid stress tensor is closed using the Sigma [15] model, which is well suited for swirled flows as it avoids the insertion of turbulent viscosity due to "solid body rotation" of the flow. The turbulence-chemistry interaction is modeled using a Thickened Flame Model (TFLES) [12] approach, which consists in artificially thickening the flame front in order to correctly solve it.
As a first step, the kinetical scheme used for methane oxydation is the reduced BFER [6] scheme, with 6 species and 2 global steps. The scheme has been built and validated for combustion simulation and no modification has been implemented to take into account possible effects of plasma on the gas chemistry.

5 Results and discussion

5.1 Cold simulation

The numerical simulation setup has been first validated by means of a cold simulation, where the burner has been run with pure air to characterize its aerodynamical behavior. The flow has been found to have a mean velocity at the exit of the injection tube of 6.15 m/s. The azimuthal mean velocity imposed by the swirler has been found to be of 4.6 m/s. This azimuthal motion centrifugates the flow and generates a vortex breakdown and the formation of an inner recirculation zone and outer recirculation zones. On the experimental side, data from a PIV measurement have been provided. A comparison of axial and azimuthal velocity profiles from the experiment and numerical simulation is shown in Fig. 6. The profiles are evaluated at a height of 4 mm from the faceplate, to ensure that the bottom end of the PIV measurement area is not influencing the results. Numerical simulation data are time and azimuthally averaged.

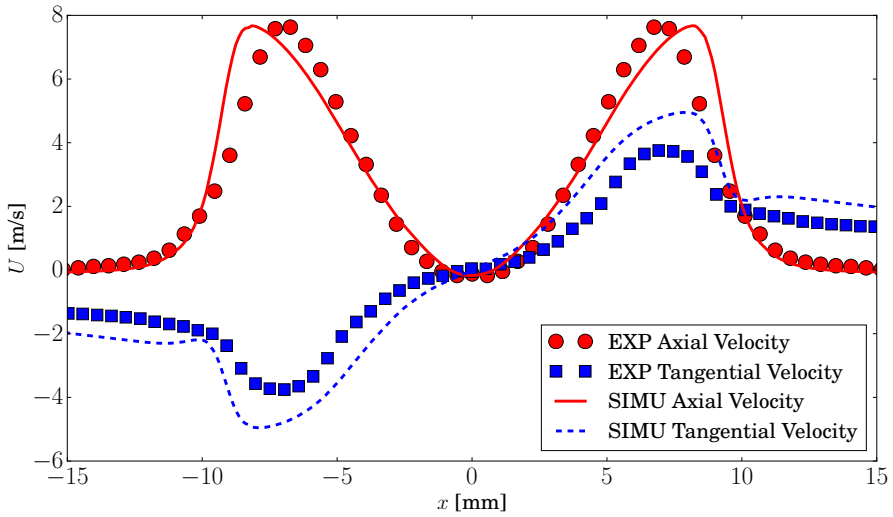

Fig. 6: Axial and azimuthal velocity profiles at a height of 4 mm from the faceplate. Comparison between experimental data collected by PIV measurements and numerical simulations.

Experimental data match well overall. The axial velocity profile perfectly reproduces the experimental one in the recirculation zone, where the same minimum of velocity is reached. Moreover the same maximum of axial velocity is also found. It can be seen however how the velocity peak is slightly shifted at an higher radial position, denoting a wider recirculation zone. This is surely linked to the azimuthal velocity profile, which exibits slightly higher values for almost all the radial components. The cause of this overestimation of the azimuthal velocity is currently under investigation. The authors are still confident that this will not be a problem in order to analyze the effect of plasma discharges on the flame: as the recirculation zone is well captured, the flame root is expected to have the right axial position.

5.2 Hot simulation without NRP discharges

Figure 7, top row, shows instantaneous temperature fields. The typical shape of a premixed flame stabilized by a swirler can be recognized. The inner recirculation zone is filled with hot combustion products (bottom row, left of Fig. 7) and serves as a heat source to ignite the fresh mixture. Outer recirculation zones, cooled down by the heat losses at walls, are filled with colder gases. The result is a V-shaped premixed flame.
Dynamically, it can be seen on the series of snapshots of Fig. 7 how the flame alternates phases in which it is attached to the pin steel electrode to phases in which it is completely lifted. This is confirmed by the field of temperature root mean square (bottom row, right of Fig. 7), which presents

large values in the zone close to the exit of the injection tube. The field of mean temperature shows how the flame shape is the one of a classical swirled flame anchored by a central recirculation zone filled with hot burnt gases. The latter has been found to extend up to the top end of the pin steel electrode.

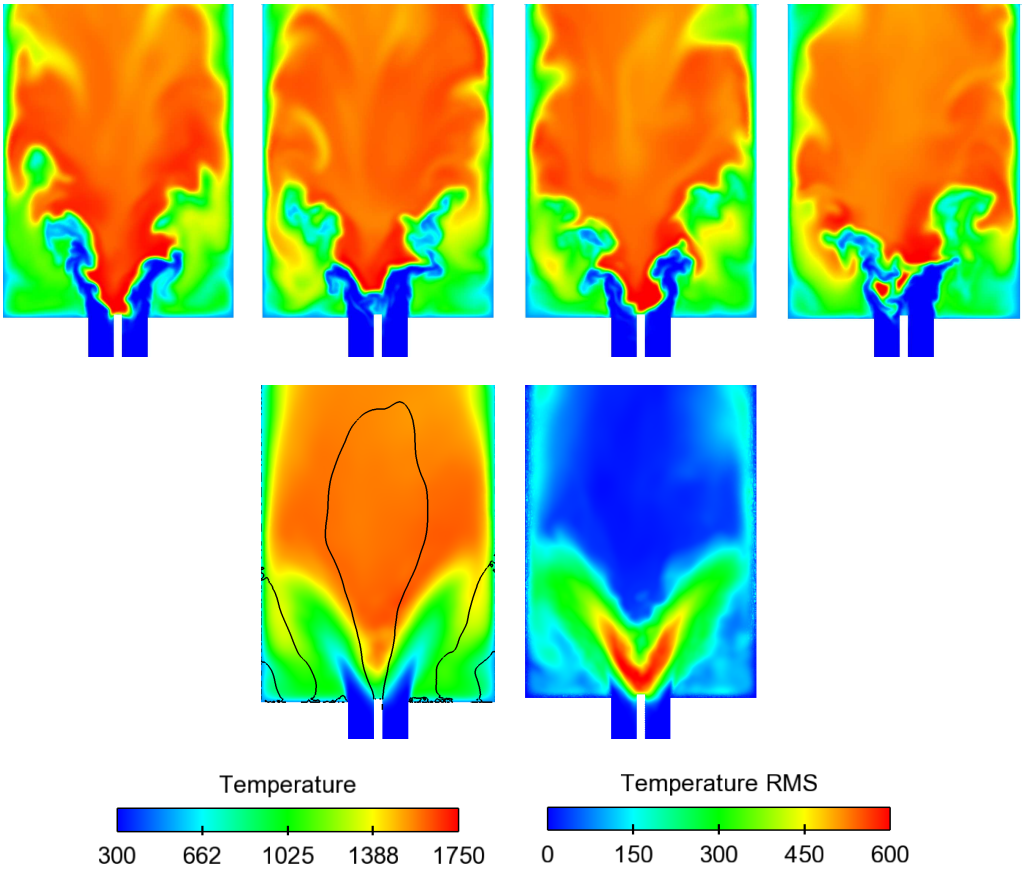

Fig. 7: Top row: snapshots of the temperature field on a longitudinal cut. Bottom row, left: mean temperature field with isolines of zero axial velocity. Bottom row, right: field of root mean square of temperature.

In order to verify if the numerical simulation is capable to retrieve the correct flame shape, the time and azimuthally-averaged field of heat release rate is compared to an image of the time-averaged Abel-inverted field of OH* emission collected in the experiment in Fig.8. It can be noticed how, qualitatively, the flame shape is very well captured by the numerical simulation and in particular how:

- both the numerical simulation and the experiment show a dispersion of the values near the top of the pin steel electrode, denoting an intermittent attached-lifted flame and a significant movement of the flame root
- the numerical simulation predicts a flame opening and flame length almost identical to the experiment
- the numerical simulation shows a larger zone of low heat release rate values compared to the experiment, especially in the flame axis, just above the flame root zone, and in the outer recirculation zones. This can be due to a slightly larger flame movement or, more probably, to a lack of information on weak light emission in the data collection of OH* emission.

5.3 Hot simulation with NRP discharges

The numerical simulations with the model developed for NRP discharges have been run using the hot simulation without NRP discharges as initial solution. Fig. 9 shows the effect of the energy

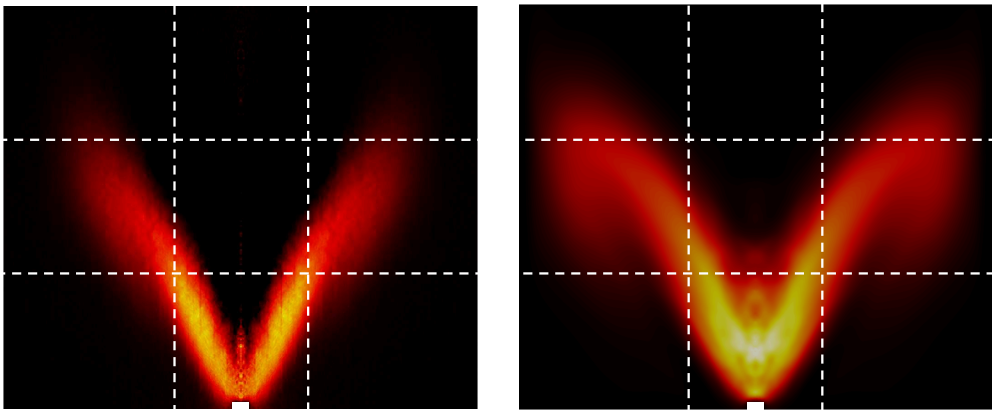

Fig. 8: Left: time-averaged Abel-inverted image of the OH* emission. Right: time and azimuthally-averaged field of the heat release rate from the numerical simulation. Both fields have been normalized by their respective maximum values.

deposit on the temperature and heat release rate fields, in a zoom around the exit of the injection tube.

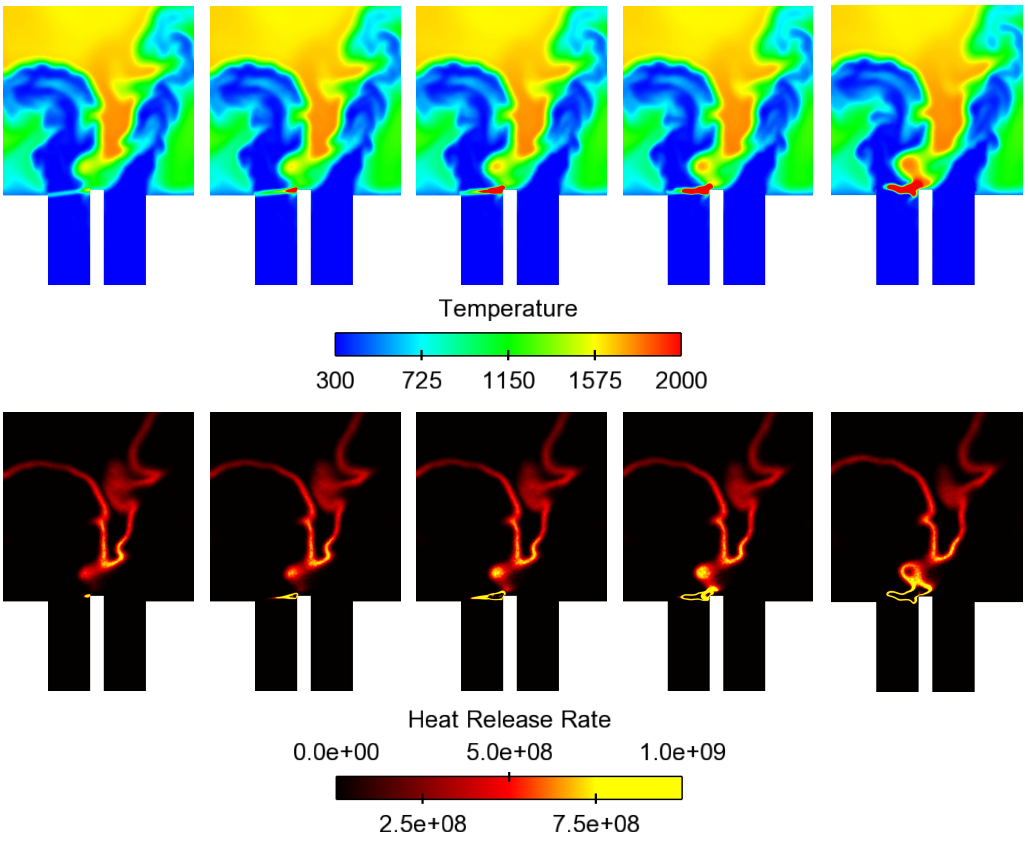

Fig. 9: Top row: temperture field with energy deposit at different instants. Bottom row: heat release rate field at the same different instants.

Starting from the left, the first three snapshots correspond to the end of the three consecutive pulses. It can be seen (top row) how the energy deposit heats up the fluid at each pulse. The very high frequency of the pulses does not give sufficient time to the heated fluid to be convected away by the flow. The second and third discharges take place in a fluid already heated, permitting to notably increase its temperature. One can notice also that, depending on the flame position, the

discharge sometimes takes place in an area where hot gases due to combustion are already present (near the pin steel electrode for instance, see the snapshot at bottom left of Fig. 9): in this case the final temperature of the fluid, which was found to be around 3000 K when starting the discharges in a gas at 300 K, can reach much higher temperatures, close to 6000-7000 K. Looking at the fields of heat release rate one can notice how the heating of the gas triggers combustion chemistry, producing heat release. At the end of the second pulse ignition appears and a flame kernel is formed. The occurrence of such event has been found to depend also on the initial gas temperature: test cases show that in a fluid at an initial temperature of 300 K the first 2 pulses produce a small amount of heat release which quickly vanishes, and that only the third pulse triggers ignition and the flame kernel formation.
The fourth and fifth snapshots of Fig. 9 show the flame kernel growth and its merging with the main flame. One has to remind that the NRP discharges turn around the pin steel electrode: the flame kernel formed by the following series of pulses is not visible in the present view but its effect on the temperature field is evident. This process anchors the flame close to the plasma discharges area and the flame apears to be much less lifted. This is confirmed in Fig. 10, to be compared with Fig. 7. The top row shows the flame topology "transformation" via snapshots of temperature field

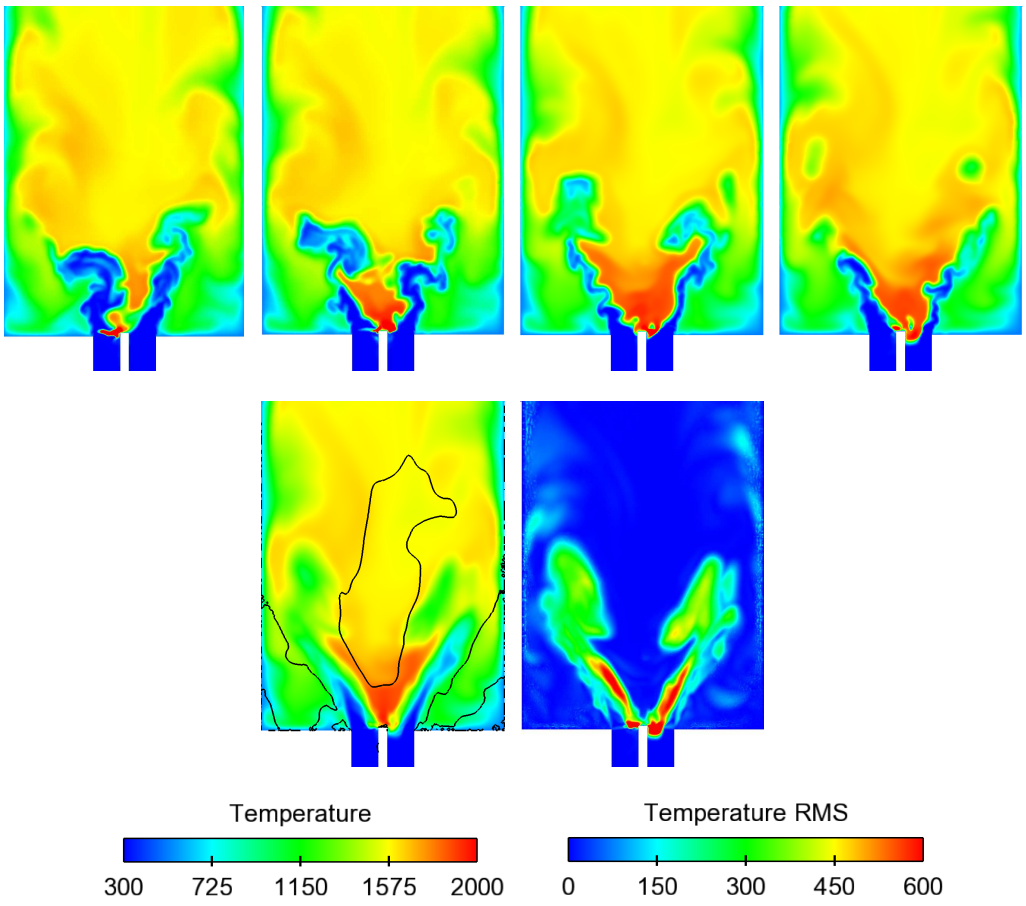

Fig. 10: Top row: snapshots of the temperature field on a longitudinal cut. Bottom row, left: mean temperature field. Bottom row, right: field of root mean square of temperature.

on a longitudinal cut. The flame, which without plasma discharges was found to intermittently attach and detach from the top of the pin steel electrode, is now always attached to it. The plasma discharges anchor the flame, which changes notably in terms of shape and dynamics. On the bottom row of one can see how the flame is less lifted in average. The mean temperature field, although still not well converged, shows how the area near the exit of the injection tube is hotter in average and provides also information on the changes this causes on the axial velocity field. Contrarily to the flame without plasma discharges, where the recirculation zone touched the top end of the

electrode, in this case the latter ends to a certain distance from it. This may suggest how the flame is now anchored not anymore by the central recirculation zone filled by hot combustion products, but by the continuous source of heating and ignition represented by the NRP discharges. The RMS temperature field shows how, even if in the discharge zone the value is strongly increased due to the intermittent pulses, the values are globally lower in the flame root zone, denoting a flame which moves less. This mechanism is promising in using NRP discharges to stabilize the flame.

6 Conclusions

A phenomenological model to describe nanosecond repetitively pulsed discharges has been built by means of experimental investigations performed at KAUST and it has been implemented in the 3D Large Eddy Simulation code AVBP, developed by CERFACS and IFPEN.
LES of a lean premixed methane-air swirl-stabilized burner have been performed, with and without NRP discharges. It has been found that, without NRP discharges, the flame is stabilized by the hot gases present in the central recirculation zone and moves around the injection tube exit zone, being more or less lifted. NRP discharges increase notably the temperature in the discharge area, leading to the triggering of chemical reactions. This promotes ignition and leads to the creation of a flame kernel. The flame kernel is then convected by the flow and merges with the main flame. This process seems to help anchoring the flame, which moves less.
Further steps will consist in increasing the complexity of the combustion kinetic scheme, which has to be adapted to high temperatures and possibly include part of the plasma chemistry. Acoustically pulsed simulations with the aim of calculating the Flame Transfer Function with and without NRP discharges are already ongoing.

References

1. Bak, M.S., Do, H., Mungal, M.G., Cappelli, M.A.: Plasma-assisted stabilization of laminar premixed methane/air flames around the lean flammability limit. Combust. Flame **159**(10), 3128–3137 (2012)
2. Barbosa, S., Pilla, G., Lacoste, D.A., Scouflaire, P., Ducruix, S., Laux, C.O., Veynante, D.: Influence of nanosecond repetitively pulsed discharges on the stability of a swirled propane/air burner representative of an aeronautical combustor. Phil. Trans. R. Soc. A **373**(2048), 20140,335 (2015)
3. Candel, S.: Combustion dynamics and control: progress and challenges. Proc. Combust. Inst. **29**(1), 1–28 (2002)
4. Castela, M., Fiorina, B., Coussement, A., Gicquel, O., Darabiha, N., Laux, C.O.: Modelling the impact of non-equilibrium discharges on reactive mixtures for simulations of plasma-assisted ignition in turbulent flows. Combust. Flame **166**, 133–147 (2016)
5. Colin, O., Rudgyard, M.: Development of high-order taylor-galerkin schemes for unsteady calculations. J. Comput. Phys. **162**(2), 338–371 (2000)
6. Franzelli, B.: Impact of the chemical description on direct numerical simulations and Large Eddy Simulations of turbulent combustion in industrial aero-engines - th/cfd/11/101. Ph.D. thesis, Université de Toulouse, France - MeGeP Dynamique des Fluides (2011)
7. Gourdain, N., Gicquel, M., Montagnac, M., Vermorel, O., Gazaix, M., Staffelbach, G., Garcia, M., Boussuge, J.F., Poinsot, T.: Comput. Sci. Disc. **2**, 015,003 (2009)
8. Huang, Y., Yang, V.: Dynamics and stability of lean-premixed swirl-stabilized combustion. Prog. Energy Comb. Sci. **35**(4), 293–364 (2009)
9. Kruger, C.H., Laux, C.O., Yu, L., Packan, D.M., Pierrot, L.: Nonequilibrium discharges in air and nitrogen plasmas at atmospheric pressure. Pure and App. Chem. **74**(3), 337–347 (2002)
10. Lacoste, D.A., Moeck, J.P., Durox, D., Laux, C.O., Schuller, T.: Effect of Nanosecond Repetitively Pulsed Discharges on the Dynamics of a Swirl-Stabilized Lean Premixed Flame. J. Eng. Gas Turb. and Power **135**(10), 101,501 (2013)
11. Lacoste, D.A., Xu, D.A., Moeck, J.P., Laux, C.O.: Dynamic response of a weakly turbulent lean-premixed flame to nanosecond repetitively pulsed discharges. Proc. Combust. Inst. **34**(2), 3259–3266 (2013)
12. Légier, J.P., Poinsot, T., Veynante, D.: Dynamically thickened flame LES model for premixed and non-premixed turbulent combustion. In: Proc. of the Summer Program , pp. 157–168. Center for Turbulence Research, NASA Ames/Stanford Univ. (2000)
13. Lieuwen, T., Yang, V.: Combustion Instabilities in Gas Turbine Engines. Operational Experience, Fundamental Mechanisms and Modeling. Prog. in Astronautics and Aeronautics AIAA Vol 210 (2005)
14. Moeck, J., Lacoste, D.A., Laux, C.O., Paschereit, C.O.: Control of combustion dynamics in a swirlstabilized combustor with nanosecond repetitively pulsed discharges. 51st AIAA Aerospace Sciences Meeting (January), AIAA–2013–565 (2013)
15. Nicoud, F., Baya Toda, H., Cabrit, O., Bose, S., Lee, J.: Using singular values to build a subgrid-scale model for large eddy simulations. Phys. Fluids **23**(8), 085,106 (2011)
16. Pancheshnyi, S.V., Lacoste, D.A., Bourdon, A., Laux, C.O.: Ignition of propane-air mixtures by a repetitively pulsed nanosecond discharge. IEEE Trans. on Pl. Sci. **34**(6), 2478–2487 (2006)

17. Pilla, G.L., Lacoste, D.A., Veynante, D., Laux, C.O.: Stabilization of a swirled propane-air flame using a nanosecond repetitively pulsed plasma. IEEE Trans. on Pl. Sci. **36**(4 PART 1), 940–941 (2008)
18. Poinsot, T.: Prediction and control of combustion instabilities in real engines. Proc. Combust. Inst. **29**, 1–29 (2017)
19. Poinsot, T., Lele, S.: Boundary conditions for direct simulations of compressible viscous flows. J. Comput. Phys. **101**(1), 104–129 (1992)
20. Schønfeld, T., Rudgyard, M.: Steady and unsteady flows simulations using the hybrid flow solver avbp. AIAA Journal **37**(11), 1378–1385 (1999)
21. Sun, W., Uddi, M., Won, S.H., Ombrello, T., Carter, C., Ju, Y.: Kinetic effects of non-equilibrium plasma-assisted methane oxidation on diffusion flame extinction limits. Combust. Flame **159**(1), 221–229 (2012)
22. Tholin, F., Lacoste, D.A., Bourdon, A.: Influence of fast-heating processes and O atom production by a nanosecond spark discharge on the ignition of a lean H2-air premixed flame. Combust. Flame (5), 1235–1246 (2014)
23. Xu, D.A., Lacoste, D.A., Laux, C.O.: Ignition of Quiescent Lean Propane-Air Mixtures at High Pressure by Nanosecond Repetitively Pulsed Discharges. Pl. Chem. and Pl. Proc. **36**(1), 309–327 (2016)